

# Time scale and freeze-out volume in the Xe + Cu reaction at 45 MeV/u

M. D'Agostino<sup>1</sup>, M. Bruno<sup>1</sup>, F. Gramegna<sup>2</sup>, I. Iori<sup>3</sup>, P.F. Mastinu<sup>1</sup>, P.M. Milazzo<sup>1</sup>, E. Plagnol<sup>4, \*</sup>, G. Vannini<sup>5</sup>

<sup>1</sup>Dipartimento di Fisica dell'Università and Istituto Nazionale di Fisica Nucleare, Via Irnerio, 46, I-40126, Bologna, Italy

<sup>2</sup>Istituto Nazionale di Fisica Nucleare, Laboratori Nazionali di Legnaro, Legnaro, Italy

<sup>3</sup>Dipartimento di Fisica dell'Università and Istituto Nazionale di Fisica Nucleare, Milano, Italy

<sup>4</sup>Laboratoire National GANIL, Caen, France

<sup>5</sup>Dipartimento di Fisica dell'Università and Istituto Nazionale di Fisica Nucleare, Trieste, Italy

Received: 9 January 1995/Revised version: 8 May 1995

Communicated by C. Signorini

**Abstract.** Correlations between Intermediate Mass Fragments were measured for the reaction Xe + Cu at  $E/A = 45$  MeV/u. The velocity correlation function for central 3-fold events, depleted at small values of the relative coordinate, as typical for fast decay processes, reflects the mutual Coulomb repulsion between the emitted fragments. From the comparisons between a significant number of experimental observables and the predictions of the Berlin Multifragmentation Model, it appears that the data are compatible with a simultaneous multifragment emission.

**PACS:** 25.70.-z

## 1. Introduction

The emission of Intermediate Mass Fragments (IMFs –  $3 \leq Z \leq 20$ ) is an important decay mechanism of the excited nuclear systems formed in heavy ion reactions at intermediate energies. The relative velocities between IMFs are a signature of the disintegration process and are a unique tool to investigate the lifetime and the density of the excited system decaying through a multifragment emission [1].

IMF–IMF correlation functions at small values of the reduced velocity [2] are controlled by the interactions between the fragments: the IMFs will move under the influence of their mutual Coulomb repulsion and will be deflected from each other, provided they are emitted in a sufficiently narrow time interval, such that their mutual distances are small. When more than two fragments are emitted, as suggested in [3], any depletion (*Coulomb hole*) in the correlation function at small reduced velocities is in contradiction with the assumption of an independent sequential fragment emission.

On the other hand, the correlation function at higher values of the reduced velocity probes the mutual

interaction between all the fragments present in the disintegration region and it is sensitive to the breakup configuration: at intermediate energies, if the disassembly occurs through the multifragmentation of the expanded nuclear system formed in central collisions, the Coulomb energy between a pair of fragments is reduced with respect to the sequential emission, leading to a smaller relative velocity.

The shape of the experimental correlation functions gives therefore significant information on the space-time evolution of the hot nuclear system [4].

The method most commonly used to extract the emission time and the dimension of the source consists in the comparison of the experimental correlation function with the prediction of three- or many-body trajectory calculations [5, 6], where the simulated events are generated from the experimental charge, energy and angular distributions and the free parameters are the size, the density and the lifetime of the emitting source. In this approach, the basic hypothesis is that IMFs are emitted sequentially from the excited and expanded source, so that their Coulomb trajectories are essentially influenced from the presence of a large residue.

A different approach is to compare the experimental correlation function with predictions of statistical decay models, based upon different assumptions such as sequential decays or instantaneous emissions, with or without the hypothesis of an expanding source [3, 7]. The information on the fragment source, obtained by this comparison, is meaningful if the model is able to reproduce all the previously mentioned experimental distributions, so that the reduced-velocity correlation function can be used to characterize the source density and the mean emission lifetime for multifragment final states.

In order to understand if also for our reaction, as for those analyzed in [5, 8], an instantaneous multifragment emission can be responsible for the observed features, in this paper we have compared IMF–IMF correlation functions to the predictions of the Berlin Multifragmentation Model (BMM) [9], which is based on a statistical and instantaneous disassembly of an expanded and excited system. It has to be noted that the simultaneous disassembly of an excited source in 3 or more fragments, like in

\* Present address: IPN Orsay, France

BMM, is compatible, as far as the relative velocities are concerned [10], with a sequential binary decay with a lifetime smaller than the Coulomb interaction time ( $\tau \approx 10^{-22}$  sec). Before comparing the correlation functions we checked that the model is able to reproduce the main features of the experimental distributions, such as charge distributions, kinetic energy and angular distribution of the IMFs. The shape of the correlation functions (in particular at low values of the reduced velocity) allows therefore to determine the density of the excited system.

## 2. Exclusive experimental observables and comparison with the model

The experiment was performed at the GANIL Laboratory bombarding a Cu target with a Xe beam at 45 MeV/u. Fragments ( $Z \geq 3$ ) were detected with the MULTICS [11–14] apparatus. The angular range covered was  $5^\circ \rightarrow 25^\circ$ , with a geometrical acceptance of 72% [15], the energy threshold was  $\approx 2.5$  MeV/u, (corresponding to a velocity  $\approx 2.2$  cm/ns, the overall energy resolution resulted better than 2% and the angular resolution ranged from  $0.1^\circ$  to  $0.3^\circ$ .

In previous papers [16, 17] we already presented part of the data and we showed that experimental inclusive observable, as the total cross section, the multiplicity distributions and the charge cross sections are well reproduced, without any normalization, by the prediction of a dynamical model based on Boltzmann, Nordheim, Vlasov (BNV) equation, followed by a statistical binary decay. However more exclusive observables, like the total charge distribution and the charge event asymmetry, were not reproduced by this *hybrid* model; indications were found of a non binary sequential decay of the hot sources formed at central impact parameters.

The *central* events, coming from the de-excitation of an equilibrated source, were identified through the fragment multiplicity and their isotropic angular distribution [17] in the centre of mass frame. The central events with three IMFs were studied and their characteristics were compared to the predictions of the BMM. A quite good agreement has been found for the event charge asymmetry  $Z_3/(Z_1 + Z_2 + Z_3)$  ( $Z_1, Z_2, Z_3$  are the heaviest, medium and lightest fragment in each event, respectively) and the distribution of the fragment total charge, using as the freeze-out radius the default one ( $r_0 \cdot A^{1/3}$  fm,  $r_0 = 2.1$  fm), if comparing 3-fold events with fragment charges  $Z \geq 6$ . The discrepancy between experimental observables and predictions for  $Z < 6$  was attributed both to experimental thresholds and to the too high production of light fragments by the BMM model. Even in the analysis presented here, the comparison between data and model predictions will be done for fragments with charge between 6 and 20.

The input parameters of the Berlin model are the mass, the atomic number, the excitation energy and the angular momentum of the source, together with the freeze-out radius. The BMM model calculates the emissions probabilities of a unique equilibrated source according to the entropy of the system. The emission is instantaneous and the fragments start their trajectories from the freeze-out configuration.

We followed the first stage of the reaction up to the time when the intermediate nuclear system has reached the equilibrium [16] with the dynamical BNV model, which takes into account momentum and energy conservation. The mean values and the variances of the mass, charge, excitation energy and angular momentum of the source, that undergoes multifragmentation, can be determined and used as inputs for the fragmentation code; only the freeze-out radius, which is a specific parameter of the Berlin model can be treated as a free parameter and its effect on the results of the calculation can be investigated through the comparison to the experimental data. For the measured reaction the source characteristics given by the dynamical BNV model for the impact parameters  $b = 0.1 \div 2$  fm are:  $A_s = 151$ ,  $Z_s = 66$ ,  $E^*/A = 5.3$  MeV/u,  $L \approx 0 \div 70 \hbar$ . In the present BMM calculations an angular momentum  $L = 11 \hbar$ , corresponding to  $b = 0.5$  fm has been used since, as discussed in the previous work [17], a larger angular momentum of the source leads to a decay in fragments with a charge asymmetry considerably higher than the experimental one. The theoretical treatment has therefore to be improved in order to reproduce the data also when the source has non negligible angular momentum, as predicted from BNV calculations for impact parameters up to 2 fm.

A software replica of the experimental apparatus was applied to the predicted events before the comparison with the experimental ones, in order to allow meaningful comparison with exclusive data. This software includes a realistic treatment of the geometrical inefficiencies, the particle kinetic energy thresholds and the particle energy loss in inactive regions [15]. The experimentally determined source velocity, used in the filtering procedure through the detecting apparatus, resulted  $\approx 7$  cm/ns, very similar to the one predicted by the incomplete fusion systematics [18], corresponding to a linear momentum transfer of 80%. Only the events detected, like the experimental ones, as 3-body events were considered in the calculation of the exclusive observables.

In Fig. 1a we present the comparison between the experimental and calculated total charge  $Z_{\text{tot}}$  of the fragments as a function of the excitation energy of the source, with the freeze-out radius at its default value  $2.1 \cdot A^{1/3}$  fm. As it is evident from this figure, the predicted total charge agrees with the experimental one in the range  $E^* = 650 \div 850$  MeV, in agreement with the BNV predicted value  $\approx 800$  MeV.

The mean value of the total charge experimentally detected is 36, i.e. 30 units of charge of the emitting source are not detected. The good agreement between the BMM calculation and the experimental value is due to the fact that in the events with 3 IMFs with  $Z \geq 6$  the BMM model predicts also 8–9 protons, 4–5  $\alpha$ -particles and 3 very light IMFs ( $3 \leq Z \leq 5$ ).

In Fig. 1b, c, d and e we show the calculated total fragment charge  $Z_{\text{tot}}$  and the charge distributions of the heaviest, medium and lightest fragment (labelled as  $Z_1, Z_2, Z_3$  respectively) as a function of the freeze-out radius, for the excitation energy values of 700 and 800 MeV. As it is clear from these plots, the freeze-out radius does not influence strongly the charge partition and the agreement between predicted and experimental charge distribution is

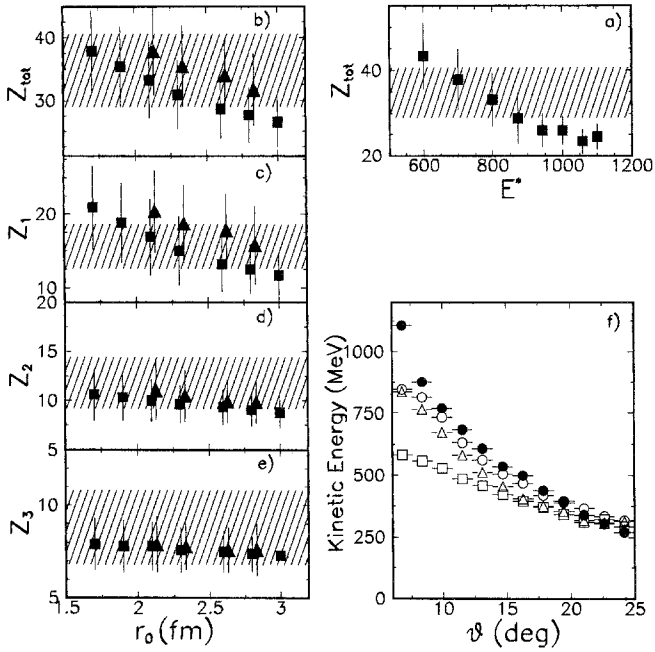


**Fig. 1.** a) Calculated (full squares) and experimental (dashed area) total charge ( $Z_{tot}$ ) of the fragments ( $Z \geq 6$ ) as a function of the excitation energy  $E^*$  of the source, for  $r_0 = 2.1$  fm. b) Calculated (full squares for an excitation energy of 800 MeV and full triangles for an excitation energy of 700 MeV) and experimental total charge  $Z_{tot}$  of the fragments ( $Z \geq 6$ ) as a function of  $r_0$ . c), d), e) Calculated and experimental charge distributions of the heaviest ( $Z_1$ ), medium ( $Z_2$ ) and lightest ( $Z_3$ ) fragments as a function of  $r_0$ . f) Laboratory mean IMF kinetic energy (MeV) versus the laboratory detection angle. The full circles refer to the experimental value, the open circles to the calculation with  $E^* = 800$  MeV and  $r_0 = 2.1$  fm, the open squares to  $E^* = 800$  MeV and  $r_0 = 2.8$  fm and the open triangles to  $E^* = 700$  MeV and  $r_0 = 2.6$  fm. The predictions were filtered by the acceptance of the apparatus

acceptable for a range  $1.9 \div 2.6 \cdot A^{1/3}$  fm of the freeze-out radius.

As claimed in [8, 19] and clearly seen in Fig. 1, increasing the excitation energy or the freeze-out radius the symmetry on the charge of the IMFs formed in the decay of the source increases. The excitation energy cannot be increased over 800 MeV since it would lead to IMFs with total detected charge  $Z_{tot}$  smaller than the experimental one; on the contrary one gets IMFs symmetric in charge, with a  $Z_{tot}$  value close to the experimental value in a wide range of the freeze-out radius.

In Fig. 1f the fragment laboratory mean kinetic energy as a function of the laboratory detection angle is reported for  $r_0 = 2.1$  fm,  $E^* = 700$  MeV, for  $r_0 = 2.6$  fm,  $E^* = 700$  MeV and for  $r_0 = 2.8$  fm  $E^* = 800$  MeV. The underestimation of the kinetic energy for the highest  $r_0$  value could be due to a missing additional energy; as it has been recently suggested [20] an additional compression energy could improve the agreement between data and model predictions as in other reactions at intermediate energies.

The overall agreement between the data and the BMM calculations allows to extend the comparison to the relative velocities distributions in order to determine the best value of the freeze-out volume which reproduces these observables. A strong influence of the freeze-out

radius is expected on the relative velocities between pairs of fragments, since the Coulomb energy depends strongly on the proximity of the fragments.

In Fig. 2a the experimental scatter plot  $V_{red}$  as a function of  $\Theta_{rel}$  for each pair of IMFs is reported.  $V_{red}$  is the reduced velocity  $V_{red} = |\vec{V}_i - \vec{V}_j| / \sqrt{(Z_i + Z_j)}$  ( $i, j = 1 \div 3, i \neq j$ ) between the IMF velocities and  $\Theta_{rel}$  is the relative angle between the IMFs velocities in the event Centre of Mass frame. In Fig. 2b, c, d the BMM predictions are reported for the excitation energy  $E^* = 800$  MeV and  $r_0 = 1.7, 2.1, 2.6$  fm respectively. The agreement with the experimental plots improves for increasing available volume, as it clearly appears from Fig. 2; an expanded source seems to be responsible for the IMFs emission.

### 3. Reduced velocity correlation functions

A more meaningful information can be extracted from the investigation of reduced velocity correlation functions, as usual in interferometry analysis [21]. The correlation functions are defined as the observed probability  $P(v_{red})$  of pairs of fragments belonging to the same event divided by the probability  $P_{mix}(v_{red})$  of uncorrelated pair of fragments with the same reduced velocity  $v_{red}$ :

$$1 + R = \frac{P(v_{red})}{P_{mix}(v_{red})}. \quad (1)$$

The uncorrelated events are obtained from the coincident events by the technique of event mixing [22], i.e. by combining fragments from different recorded events. Mixed events take into account (as the correlated ones) the efficiency and the finite granularity of the experimental apparatus: events where two mixed fragments could have been detected in the same detector were rejected. This request is needed when calculating correlation functions for IMF, especially when dealing with reverse kinematics experiments; in fact, due to kinematical constraints, the detection angles of the fragments are limited in a forward cone and the probability of double counting, when mixing the events, depends on the number of detectors used to cover these angles. If one does not apply the rejection of the double hits, the uncorrelated probability  $P_{mix}(v_{red})$  in the equation (1) is increased at low reduced velocities and, due to the normalization over the whole area, the correlation function is enhanced at higher values of the reduced velocity, simulating additional correlations. The yield of the double hits for the correlated and uncorrelated events, estimated by filtering BMM calculations, is of the order of 4% and 13.5% respectively. It has to be noted that no arbitrary normalization is used, since expression (1) defines uniquely the normalization of the correlation functions [8].

In Fig. 3 the experimental correlation functions of the reduced velocity are shown, together with the calculated ones for  $E^* = 800$  MeV and  $r_0 = 1.7, 2.1, 2.8$  fm and for  $E^* = 700$  MeV and  $r_0 = 2.6$  fm. The error bars of the experimental data correspond to the statistical error on the correlated yield; the high number of mixed events does not affect the correlation function errors.

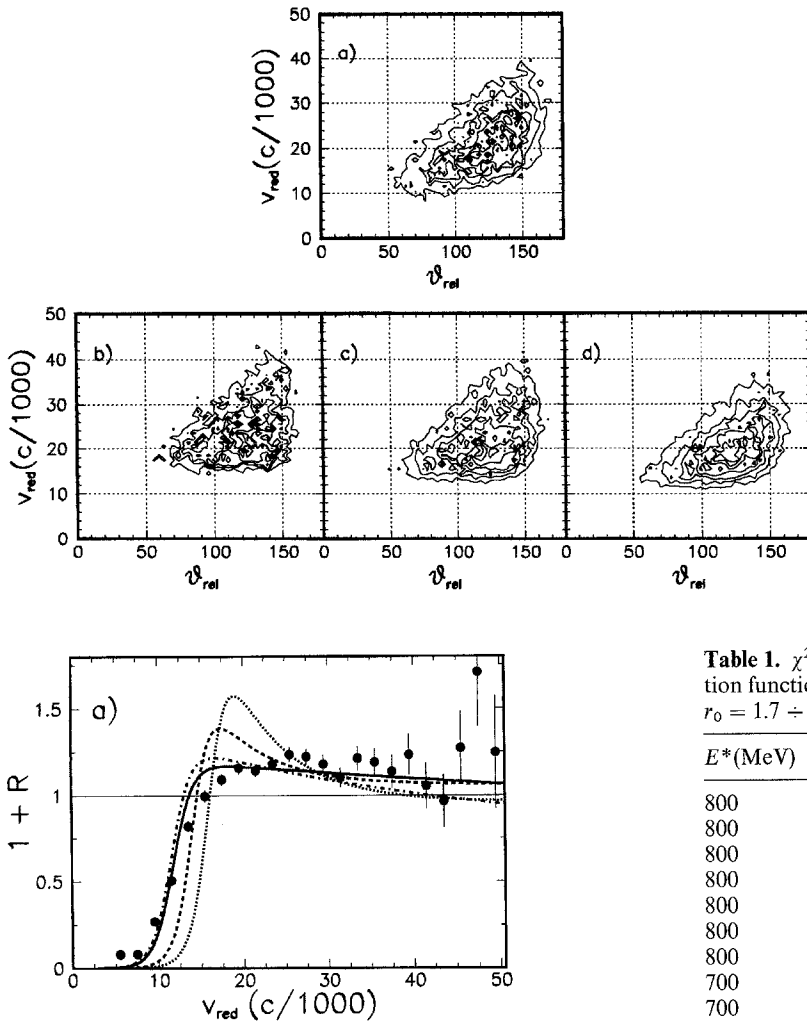


**Fig. 3.** Correlation functions of the reduced velocity. The *full line* is the predicted correlation functions for  $r_0 = 2.8$  fm and the excitation energy  $E^* = 800$  MeV. The *dashed*, *dotted* and *dash-dotted lines* are the predicted values for  $r_0 = 2.1$  fm and  $E^* = 800$  MeV,  $r_0 = 1.7$  fm and  $E^* = 800$  MeV, and  $r_0 = 2.6$  fm and  $E^* = 700$  MeV, respectively, fitted following the procedure described in [23]. The predictions were filtered by the acceptance of the apparatus

The evident depletion in Fig. 3 at low values of the reduced velocity in the experimental data is a signature of a short decay time: the fragment emission is fast enough to have noticeable mutual Coulomb interaction between IMF after their separation.

The bump of the calculated correlation function of the reduced velocity, just after the *Coulomb hole*, decreasing with increasing  $r_0$ , reflects the modification of the charge partition and of the breakup configuration. As it can be seen from Fig. 1, indeed, the charge partition evolves towards an increasing symmetry with  $r_0$ , due to the increase of the free volume. At low  $r_0$  values, when the largest fragment ( $Z_1$ ) is much larger than the other IMFs, the smaller ones ( $Z_2$  and  $Z_3$ ) are at the maximum distance from the largest one because of the Coulomb repulsion. The resulting relative motion of  $Z_2$  and  $Z_3$  will be governed more by their mutual repulsion than by the interaction with the largest fragment [19]. This leads to a pair of IMFs ( $Z_2, Z_3$ ) with relatively high relative velocity and two

**Fig. 2a–d.** Contour plot of the reduced velocity  $v_{red}$  vs. relative angle ( $\theta_{rel}$ ) between couples of IMFs: a) experimental; b), c), d) BMM prediction for  $E^* = 800$  MeV and  $r_0 = 1.7$  fm and  $r_0 = 2.1$  fm and  $r_0 = 2.6$  fm, respectively.

**Table 1.**  $\chi^2$  of the IMF-IMF ( $6 \leq Z \leq 20$ ) reduced velocity correlation functions with respect to the prediction of the Berlin model, for  $r_0 = 1.7 \div 3.0$  fm and  $E^* = 700, 800$  MeV

$E^*$ (MeV)	$r_0$ (fm)	$\chi^2$
800	1.7	22.1
800	1.9	14.9
800	2.1	9.0
800	2.3	5.2
800	2.6	2.6
800	2.8	2.2
800	3.0	2.4
700	2.1	9.0
700	2.3	7.0
700	2.6	5.2
700	2.8	4.0

pairs ( $Z_1, Z_2$  and  $Z_1, Z_3$ ) with lower relative velocities. Events with IMFs asymmetric in charge contribute to the correlation functions twice at low values of the relative velocity and once at higher values of the abscissa; this is the origin of the bump in the calculated correlation function after the *Coulomb hole* for low  $r_0$  values. At higher  $r_0$  values, due to the increasing of the free volume, more symmetric charge partitions are available; this reflects in a flatter correlation function (see Fig. 3).

We investigated how the experimental uncertainties and finite resolution effects reflect on the *Coulomb hole* and on the shape of the correlation functions. We found that, in our case, the low velocity threshold ( $\approx 2$  cm/ns), the energy resolution (better than 2%) and the angular one ( $0.1^\circ \rightarrow 0.3^\circ$ ) lead to an overall error on the reduced abscissa  $\approx 5\%$ . The correlation function is then only slightly affected by the acceptance of the apparatus and therefore the observed *Coulomb hole* cannot be attributed to experimental limitations.

In Table 1 we present  $\chi^2 = 1/N_{\text{points}} (\sum (f_{th}(v_{red}) - f_{exp}(v_{red}))^2 / \text{err}_{exp}^2(v_{red}))$ , the normalized distance of the experimental correlation function with respect to the predicted values for several combination of the freeze-out radius and of the excitation energies.

From Figs. 2, 3 and from Table 1 it is evident that the best agreement between the data and the calculations is obtained for the largest values ( $2.6 \div 3.0$  fm) or  $r_0$  for an excitation energy of 800 MeV. Since however, as it can be seen in Fig. 1f), with these inputs the kinetic energies are underestimated, an overall better reproduction of all the observables seems to be obtained for a lower excitation energy (700 MeV) and for a freeze-out radius of the order of ( $2.6 \div 2.8A^{1/3}$  fm).

#### 4. Conclusions

The experimental correlation function of the events with 3 IMF's, showing a clear *Coulomb hole*, indicates that the decay of the system formed in central collisions is a very fast process compared with the Coulomb interaction time ( $\tau \approx 10^{-22}$  sec) and, as stressed in [3] rules out conventional sequential binary decay models which use independent decay rates for subsequent decays. The agreement between the experimental data and the prediction of the BMM model and the comparison of the correlation functions indicate that the multifragment production observed in central collisions in the reaction Xe + Cu at 45 MeV/u can be explained within the BNV + BMM approach with a freeze-out radius  $2.6 \div 2.8A^{1/3}$  fm and an excitation energy  $\approx 4.6 \div 5.3$  MeV/u. The mechanism for multifragment production, if one selects the most central collisions, is compatible with an instantaneous breakup of the intermediate excited system.

The authors would like to thank A. Bonasera, M. Di Toro, D.E. Gross and O. Schapiro for many interesting and stimulating discussions and for making their codes available and the MULTICS group for the collaboration in the measurements. Fruitful discussions with Wolfgang Trautmann and Adriano Gobbi are gratefully acknowledged. This work has been supported in part by funds of the Italian Ministry of University and Scientific Research.

#### References

1. R. Trockel, U. Lynen, J. Pochodzalla, W. Trautmann, N. Brummund, E. Eckert, R. Glasow, K.D. Hildenbrand, K.H. Kampert, W.F.J. Müller, D. Pelte, H.J. Rabe, H. Sann, R. Santo, H. Stelzen, R. Wada, Phys. Rev. Lett. **59**, 2844 (1987); R. Bougault, J. Colin, F. Delaunay, A. Genoux-Lubain, A. Hajfani, C. Le Brun, J.F. Lecolley, M. Louvel, J.C. Steckmayer, Phys. Lett. **B232**, 291 (1989); M. Louvel, A. Genoux-Lubain, G. Bizard, R. Bougault, R. Brou, A. Buta, H. Doubre, D. Durand, Y. El Masri, H. Fugiwara, K. Hagel, T. Hamdani, F. Hanappe, S.C. Jeong, G.M. Jim, S. Kata, J.L. Laville, C. Le Brun, J.F. Lecolley, S.M. Lee, T. Matsuse, T. Motobayashi, A. Péghaire, J. Péter, R. Régimbart, F. Saint-Laurent, J.C. Steckmayer, B. Tamain, Phys. Lett. **B320**, 221 (1994).
2. J. Pochodzalla, Proceedings of the International School of Physics "Enrico Fermi"-Course XII-Edited by C. Detraz and P. Kienle, Varenna 1989.
3. O. Schapiro and D.H.E. Gross, Nucl. Phys. **A576**, 428 (1994).
4. see for instance: D. Fox, R.T. de Souza, L. Phair, D.R. Bowman, N. Carlin, C.K. Gelbke, W.G. Gong, Y.D. Kim, M.A. Lisa, W.G. Lynch, G.F. Peaslee, M.B. Tsang, F. Zhu, Phys. Rev. C **47**, R421 (1993); E. Bauge, A. Elmaani, Roy A. Lacey, J. Lauret, N.N. Ajitanand, D. Graig, M. Cronqvist, E. Gualtieri, S. Hannuschke, T. Li, B. Llope, T. Reposeur, A. Vander Molen, G.D. Westfall, J.S. Winfield, J. Yee, S. Yennello, A. Nadasen, R.S. Tinkle, E. Norbeck, Phys. Rev. Lett. **70**, 3705 (1993); D. Guerreau Nucl. Phys. **A574**, 111c (1994).
5. D.R. Bowman, G.F. Peaslee, N. Carlin, R.T. de Souza, C.K. Gelbke, W.C. Gong, Y.D. Kim, M.A. Lisa, W.G. Lynch, L. Phair, M.B. Tsang, C. Williams, N. Colonna, K. Hanold, M.A. McMahan, G.J. Wozniak and L.G. Moretto, Phys. Rev. Lett. **70**, 3534 (1993).
6. Y.D. Kim, R.T. de Souza, D.R. Bowman, N. Carlin, C.K. Gelbke, W.G. Gong, W.G. Lynch, L. Phair, M.B. Tsang, F. Zhu, Phys. Rev. C **45**, 338 (1992); Y.D. Kim, R.T. de Souza, C.K. Gelbke, W.G. Gong, S. Pratt, Phys. Rev. C **45**, 387 (1992); T. Glasmacher, L. Phair, D.R. Bowman, C.K. Gelbke, W.G. Gong, Y.D. Kim, M.A. Lisa, W.G. Lynch, G.F. Peaslee, M.B. Tsang, F. Zhu, Phys. Rev. C **50**, 952 (1994).
7. O. Lopez, M. Aboufiriassi, A. Badala, B. Bilwes, R. Bougault, R. Brou, J. Colin, F. Cosmo, D. Durand, A. Genoux-Lubain, D. Horn, J.L. Laville, C. Le Brun, J.F. Lecolley, F. Lefebvres, M. Louvel, M. Mahi, C. Paulot, A. Peghaire, G. Rudolf, F. Scheibling, J.C. Steckmayer, L. Stuttge, B. Tamain and S. Tomasevic, Phys. Lett. **B315**, 34 (1993).
8. O. Schapiro, A.R. DeAngelis, D.H.E. Gross, Nucl. Phys. **A568**, 333 (1994).
9. D.H.E. Gross, X. Zhang, and S. Xu, Phys. Rev. Lett. **56**, 1544 (1986); X.Z. Zhang, D.H.E. Gross, S. Xu, and Y.M. Zheng, Nucl. Phys. **A461**, 668 (1987); D.H.E. Gross, Rep. Prog. Phys. **A53**, 605 (1990).
10. M. Bruno, M. D'Agostino, M.L. Fian dri, E. Fuschini, P.M. Milazzo, A. Cunsolo, A. Foti, F. Gramegna, I. Iori, L. Manduci, A. Moroni, P. Buttazzo, G.V. Margagliotti and G. Vannini, Nuovo Cim. **105A**, 1629 (1992).
11. I. Iori, L. Manduci, A. Moroni, R. Scardaoni, Sun Chong Wen, Zhang Yuzhao, Zhang Guangming, F. Giglio, E. Mora, G. Di Pietro, L. Delleria, A. Cortesi, R. Bassini, C. Boiano, S. Brambilla, M. Malatesta, M. Bruno, M. D'Agostino, M.L. Fian dri, E. Fuschini, P.M. Milazzo, G. Busacchi, A. Cunsolo, A. Foti, G. Sava, F. Gramegna, P. Buttazzo, G.V. Margagliotti and G. Vannini, Nucl. Instr. and Meth. **A325**, 458 (1993).
12. M. Bruno, M. D'Agostino, M.L. Fian dri, E. Fuschini, P.M. Milazzo, S. Ostuni, F. Gramegna, I. Iori, L. Manduci, A. Moroni, R. Scardaoni, P. Buttazzo, G.V. Margagliotti and G. Vannini, Nucl. Instr. and Meth. **A311**, 189 (1992).
13. N. Colonna, G.J. Wozniak, A. Veeck, W. Skulski, G.W. Goth, L. Manduci, P.M. Milazzo and P.F. Mastinu, Nucl. Instr. and Meth. **A321**, 529 (1992).
14. P.F. Mastinu, P.M. Milazzo, M. Bruno, M. D'Agostino, L. Manduci, Nucl. Instr. and Meth. **A338**, 419 (1994).
15. M. Bruno, M. D'Agostino, P.M. Milazzo, S. Ostuni, E. Fuschini and A. Moroni, Nucl. Instr. and Meth. **A305**, 410 (1991).
16. M. Bruno, M. D'Agostino, M.L. Fian dri, E. Fuschini, P.M. Milazzo, A. Cunsolo, A. Foti, F. Gramegna, F. Gulminelli, I. Iori, L. Manduci, A. Moroni, R. Scardaoni, P. Buttazzo, G.V. Margagliotti, G. Vannini, G. Auger and E. Plagnol, Phys. Lett. **B292**, 251 (1992).
17. M. Bruno, M. D'Agostino, M.L. Fian dri, E. Fuschini, L. Manduci, P.F. Mastinu, P.M. Milazzo, F. Gramegna, A.M.J. Ferrero, F. Gulminelli, I. Iori, A. Moroni, R. Scardaoni, P. Buttazzo, G.V. Margagliotti, G. Vannini, G. Auger, E. Plagnol, Nucl. Phys. **A576**, 138 (1994).
18. V.E. Viola Jr., B.B. Back, K.L. Wolf, T.C. Awes, C.K. Gelbke and H. Breuer, Phys. Rev. C **26**, 178 (1982).
19. O. Schapiro and D.H.E. Gross, Proceedings of the International Workshop XXII on Gross Properties of Nuclei and Nuclear Excitation; Hirscheegg, Austria, January 17-22, 1994, page 82.
20. M. Aboufiriassi, A. Badala, B. Bilwes, G. Bizard, R. Bougault, R. Brou, F. Cosmo, J. Colin, D. Durand, J. Galin, A. Genoux-Lubain, D. Guerreau, T. Hamdani, D. Horn, D. Jacquet, J.L. Laville, J.F. Lecolley, F. Lefebvres, C. Le Brun, O. Lopez, M. Louvel, M. Mahi, M. Morjean, A. Péghaire, J. Péter, R. Régimbart, G. Rudolf, F. Scheibling, J.C. Steckmayer, L. Stuttgé, B. Tamain and S. Tomasevic, XXXII International Winter

Meeting on Nuclear Physics, Bormio, January 1994, ed. by I. Iori, Ric. Sc. and E.P. **97**, 1 (1994); R. Bougault, M. Aboufiriassi, A. Badala, R. Brou, J. Colin, D. Durand, A. Genoux-Lubain, D. Horn, J.L. Laville, C. Le Brun, J.F. Lecolley, F. Lefebvres, O. Lopez, M. Louvel, M. Mahi, C. Paulot, J.C. Steckmayer, B. Tamain, B. Bilwes, F. Cosmo, G. Rudolf, F. Scheibling, L. Stuttgé, A. Péghaire, XXXII International Winter Meeting on Nuclear Physics, Bormio, January 1994, ed. by I. Iori, Ric. Sc. and E.P. **97**, 28 (1994).

21. see for instance: A Elmaani, N.N. Ajitanand, J.M. Alexander, R. Lacey, S. Kox, E. Liatard, F. Merchez, T. Motobayashi, B. Noren, C. Perrin, D. Rebreyend, Tsan Ung Chen, G. Auger, S. Groult, Phys. Rev. C **43**, R2474 (1991).
22. D. Drijard, H.G. Fisher and T. Nakada, Nucl. Instr. and Meth. **225**, 367 (1984).
23. T.C. Sangster, M. Begemann-Blaich, Th. Blaich, H.C. Britt, A. Elmaani, N.N. Ajitanand, M.N. Namboodiri, Phys. Rev. C **47**, R2457 (1993).